The Plant Cell, Vol. 18, 1226–1238, May 2006, www.plantcell.org

The Plastid Protein THYLAKOID FORMATION1 and the Plasma Membrane G-Protein GPA1 Interact in a Novel Sugar-Signaling Mechanism in *Arabidopsis* [W]

Jirong Huang,[a,1,2] J. Philip Taylor,[a,1] Jin-Gui Chen,[a,3] Joachim F. Uhrig,[b,4] Danny J. Schnell,[c] Tsuyoshi Nakagawa,[d] Kenneth L. Korth,[e] and Alan M. Jones[a,f,5]

[a] Department of Biology, University of North Carolina, Chapel Hill, North Carolina 27599
[b] Max Planck Institute for Plant Breeding Research, D-50829 Cologne, Germany
[c] Department of Biochemistry and Molecular Biology, University of Massachusetts, Amherst, Massachusetts 01003
[d] Research Institute of Molecular Genetics, Shimane University, Matsue 690-8504, Japan
[e] Department of Plant Pathology, University of Arkansas, Fayetteville, Arkansas 72701
[f] Department of Pharmacology, University of North Carolina, Chapel Hill, North Carolina 27599

Mutations in genes encoding components of the heterotrimeric G-protein complex were previously shown to confer altered sensitivity to increased levels of D-glucose. This suggests that G-protein coupling may be a novel sugar-signaling mechanism in *Arabidopsis thaliana*. THYLAKOID FORMATION1 (THF1) is here demonstrated in vivo as a Gα interaction partner that functions downstream of the plasma membrane–delimited heterotrimeric G-protein (GPA1) in a D-glucose signaling pathway. THF1 is a plastid protein localized to both the outer plastid membrane and the stroma. Contact between root plastidic THF1 and GPA1 at the plasma membrane occurs at sites where the plastid membrane abuts the plasma membrane, as demonstrated by Förster resonance energy transfer (FRET). A probable role for THF1 in sugar signaling is demonstrated by both biochemical and genetic evidence. Root growth in the *thf1-1* null mutant is hypersensitive to exogenous D-glucose, and *THF1*-overexpressing roots are resistant to inhibition of growth rate by high D-glucose. Additionally, THF1 levels are rapidly degraded by D-glucose but not L-glucose. The interaction between THF1 and GPA1 has been confirmed by in vitro and in vivo coimmunoprecipitation, FRET analysis, and genetic epistasis and provides evidence of a sugar-signaling mechanism between plastids and the plasma membrane.

INTRODUCTION

D-Glucose, a vital cellular nutrient, serves as both a source of energy and a substrate. Not surprisingly given its paramount role, D-glucose also causes a number of hormone-like responses in a variety of eukaryotes, affecting the regulation of gene expression and developmental processes (Sheen et al., 1999; Rolland et al., 2001). Because all plants both produce and use D-glucose, they must be capable of specifically adapting to changing levels of this hexose. The mechanisms of D-glucose signaling in plants are largely unknown, but one involves at least in part a hexokinase-metabolizing D-glucose transported into cells (Sheen et al., 1999; Rolland et al., 2001; Moore et al., 2003).

There is emerging evidence that other sugar-signaling mechanisms exist in plants and yeast (Rolland et al., 2001; Eastmond and Graham, 2003; Tiessen et al., 2003; Kolbe et al., 2005), including a hexokinase-independent mechanism involving key components of the G-protein heterotrimer (Ullah et al., 2002; Chen et al., 2003; Chen and Jones, 2004). This is not without precedent, as a G-protein–coupled D-glucose signaling mechanism was recently identified in the yeast *Saccharomyces cerevisiae*, in which it has been shown that sugar agonists and antagonists bind with low affinity to Gpr1, a G-protein–coupled receptor (GPCR) (Lemaire et al., 2004). This, in turn, initiates cyclic AMP signaling in a pathway involving protein kinase A, a G-protein α subunit, and a regulator of G-protein signaling (RGS) protein (Colombo et al., 1998; Versele et al., 1999).

It is well established that the *Arabidopsis thaliana* genome encodes a single canonical Gα subunit (GPA1) (Ma et al., 1990; Ullah et al., 2001), a single Gβ subunit (AGB1) (Weiss et al., 1994), two Gγ subunits (AGG1 and AGG2) (Mason and Botella, 2000, 2001), and a single RGS protein (RGS1) (Chen et al., 2003). By contrast, there are an estimated 23 Gα, 6 Gβ, and 12 Gγ subunit genes in mammals (Vanderbeld and Kelly, 2000) and 37 RGS

[1] These authors contributed equally to this work and are listed alphabetically.
[2] Current address: Shanghai Institute of Plant Physiology and Ecology, Chinese Academy of Sciences, 300 Fenglin Road, Shanghai 200032, China.
[3] Current address: Department of Botany, University of British Columbia, 6270 University Boulevard, Vancouver, BC V6T 1Z4, Canada.
[4] Current address: University of Cologne, Department of Botany III, Gyrhofstrasse 15, D-50931 Cologne, Germany.
[5] To whom correspondence should be addressed. E-mail alan_jones@unc.edu; fax 919-962-1625.
The author responsible for distribution of materials integral to the findings presented in this article in accordance with the policy described in the Instructions for Authors (www.plantcell.org) is: Alan M. Jones (alan_jones@unc.edu).
[W] Online version contains Web-only data.
Article, publication date, and citation information can be found at www.plantcell.org/cgi/doi/10.1105/tpc.105.037259.

proteins (Siderovski and Willard, 2005), making *Arabidopsis* an advantageous model system for the study of G-protein–coupled signaling (Jones and Assmann, 2004). However, a plant GPCR, with its cognate ligand activating the plant G-protein complex, has not been identified, although candidate GPCRs have been proposed (Devoto et al., 1999; Pandey and Assmann, 2004). Furthermore, signaling elements activated by plant G-proteins (i.e., effectors) are few (Jones and Assmann, 2004). To date, only two candidate effectors have been shown to interact with GPA1 in vitro: one interaction suggests a role for heterotrimeric G-proteins in the regulation of germination and seedling development (Lapik and Kaufman, 2003), and the other demonstrates the regulation of phospholipase D activity, possibly via interaction at a DRY motif similar to that found in G-protein–coupled receptors (Zhao and Wang, 2004).

Despite the apparent lack of information about the components of G-protein signaling mechanisms, this linchpin element has been implicated in a wide array of signals in plants (Wang et al., 2001; Ullah et al., 2002, 2003; Booker et al., 2004; Joo et al., 2005). Thus, in plants, mutant analyses have shown that heterotrimeric G-proteins represent a critical nexus in the signal regulation of a variety of processes such as germination, cell division and elongation, stress responses, and plant morphology (Perfus-Barbeoch et al., 2004). As such, the field is wide open for the identification of novel interaction partners for Gα.

Because null mutations in *GPA1* and *RGS1* have been shown to confer altered sensitivities to D-glucose (Ullah et al., 2002; Chen et al., 2003; Chen and Jones, 2004), we explored the mechanism of G-protein–coupled D-glucose signaling in *Arabidopsis*. Because the main target of RGS1 is the activated GTP-bound form of GPA1 ($GPA1^{GTP}$) (Chen et al., 2003) and because we have shown that the activated form of GPA1 can confer sugar resistance (this study), we sought physical interactors to $GPA1^{GTP}$ as potential effectors or modifiers in G-protein–coupled sugar signaling. We identified a GPA1-interacting protein designated THYLAKOID FORMATION1 (THF1) (Wang et al., 2004), and through both biochemical and genetic approaches, we provide evidence that THF1 functions as a downstream component of the *Arabidopsis* G-protein–coupled sugar-signaling pathway.

Here, we show that THF1 is ubiquitously expressed in *Arabidopsis*, with the highest *THF1* promoter:β-glucuronidase (GUS) activity observed in root meristems. THF1 is localized to the outer plastid membrane and/or the plastid stroma and is also found in plastid stromules. Although the concept of extraplastidic signaling via stromules interacting with the plasma membrane was revisited recently (Kwok and Hanson, 2004a, 2004b, 2004c), this work demonstrates a specific signaling event between the plastid and the plasma membrane that represents a novel sugar-signaling mechanism in eukaryotic cells.

RESULTS

The *Arabidopsis* Heterotrimeric G-Protein Is Involved in Sugar Signaling in the Root

Previously, we and others have shown that *gpa1* null seedlings were more sensitive to increased levels of D-glucose, but not mannitol, during germination (Ullah et al., 2002; Chen et al., 2006) and that *gpa1* null seedlings were hypersensitive to D-glucose (Chen et al., 2003) in a green-seedling assay (Jang et al., 1997). As the highest levels of *GPA1* expression are observed in roots, we investigated the effects of increased D-glucose during root development. Seeds of wild-type (Columbia) and *gpa1-4* plants were germinated on medium containing either control (1%) or increased (6%) D-glucose or 6% mannitol as an osmotic control. The growth rate of the primary roots of these seedlings was assayed daily for 6 d, starting 48 h after the plates were placed in the light.

Consistent with previous findings using the green-seedling and germination assays (Ullah et al., 2002; Chen et al., 2003), plants lacking GPA1 were more sensitive to D-glucose. The growth rate of the primary root was reduced in *gpa1-4* seedlings exposed to 6% D-glucose (Figure 1A, middle panel) in the days after germination but was not statistically different from the wild-type growth rate on the control level of 1% D-glucose. The retardation in root growth was relieved upon return to 1% D-glucose–containing plates (data not shown). Importantly, both wild-type and *gpa1-4* seedlings were observed to be similarly sensitive to the 6% mannitol levels, confirming that the growth-arrest phenotype observed on increased D-glucose was not attributable to an osmotic effect.

We confirmed a role for GPA1 in sugar signaling through an analysis of plants overexpressing a constitutively active form of GPA1 [$GPA1^{(Q222L)}$]. Seedlings overexpressing $GPA1^{(Q222L)}$ have previously been shown to have other growth phenotypes, similar to *rgs1-2* null seedlings (Chen et al., 2003). Root growth in seedlings from two lines overexpressing $GPA1^{(Q222L)}$ was compared with that in wild-type Wassilewskija (Ws). As shown in Figure 1B, the two $GPA1^{(Q222L)}$ transgenic lines (D and E) exhibited greater resistance to high D-glucose compared with wild-type Ws, indicating a role for the GTP-bound form of Gα ($GPA1^{GTP}$) in overcoming increased D-glucose levels.

THF1 Is a GPA1 Interaction Partner

As shown in Figure 1B, overexpression of a constitutively active form of GPA1 conferred tolerance to increased levels of D-glucose. This demonstrates a role for G-protein–coupled signaling, and more specifically, $GPA1^{GTP}$, in mediating *Arabidopsis* responses to high D-glucose. Therefore, to identify potential downstream components of this pathway, we sought effectors that interact with $GPA1^{(Q222L)}$ as bait in a yeast two-hybrid screen (Figure 2).

We screened three yeast cDNA libraries constructed from different *Arabidopsis* tissues using both low- and high-copy versions of the bait and focused on a candidate clone that was subsequently confirmed to encode an interactor in the yeast two-hybrid configuration by recloning and retesting and by coimmunoprecipitation experiments (Figures 2A, 2B, and 2D). We demonstrated that the full-length protein interacts with GPA1 in the presence of both GDP and GTPγS. The prey encodes the 162–amino acid C-terminal sequence of a 300–amino acid protein (At2g20890), which we previously designated THF1 (Wang et al., 2004). As we reported previously (Wang et al., 2004), THF1 does not share significant sequence with any known protein, but similar proteins can be found in a number of other

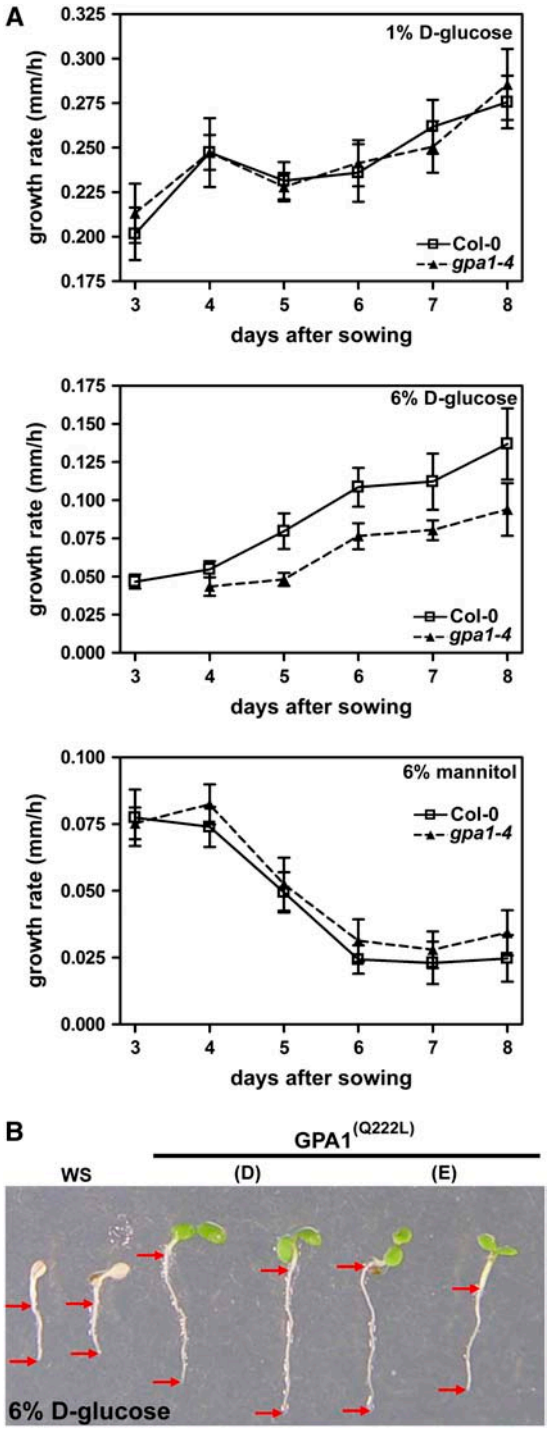

Figure 1. Heterotrimeric G-Protein α Subunit Is Involved in Sugar Signaling.

(A) Seedlings of wild-type Columbia (Col-0) and *gpa1-4* genotypes were sown on normal (1%) and increased (6%) D-glucose and 6% mannitol as an osmotic control. The rate of growth of the primary root was assayed over a 6-d period, beginning 48 h after exposure to light. Shown are interval growth rates for each 24-h period expressed as millimeters of growth per hour. Error bars represent SE. $n > 10$. As shown previously by Ullah et al. (2002), *gpa1* mutants have delayed germination on high glucose. Student's *t* tests were performed with pairwise comparison between wild-type and mutant root growth rate on 6% D-glucose. For days 5 and 6, $P < 0.1$; for days 4, 7, and 8, $P = \sim 0.2$.

(B) Seedlings overexpressing the constitutively active form of the Gα subunit [$GPA1^{(Q222L)}$] are less sensitive to increased D-glucose than are wild-type seedlings. Images show 7-d-old seedlings. Arrows denote root tips and root/shoot junctions.

species, with potato (*Solanum tuberosum*) and rice (*Oryza sativa*) proteins shown for comparison (Figure 2C). Additional analyses predicted the three-dimensional folding structure to be weakly supported as an ENTH fold, as found in the human inositol triphosphate binding, clathrin assembly protein (clathrin assembly lymphoid myeloid leukemia, Q13492). However, no binding to a lipid profile (PIP Stips P-6001; Echelon Bioscience) was observed. Nonetheless, the predicted analogy is consistent with the observed altered membrane trafficking in our previous study (Wang et al., 2004).

As shown in Figure 2C, inspection revealed that THF1 has four stretches of low similarity to M repeats such as M6_STRPY from *Streptococcus pyogenes* (Fischetti, 1989), a motif found within protein interaction interfaces (bars). The interaction region between THF1 and GPA1, which lies within the C-terminal 162 amino acids of THF1, encompasses at least three of the four putative M repeats. The conserved Leu residues highlighted in Figure 2C (dots) are suggested to be important for coiled-coil secondary structure (Herwald et al., 2004).

We tested the interaction between GPA1 and full-length THF1 by an in vitro coprecipitation assay (Figure 2B). For this purpose, 6xHis-GPA1 and GST-THF1 were expressed and purified from *Escherichia coli* using nickel and glutathione *S*-transferase (GST) columns, respectively. To determine whether THF1 interacts preferentially with the GTP-bound form of GPA1, GPA1 was loaded with GDP or GTPγS before adding GST-THF1 to the binding assay buffer. We detected a qualitatively similar binding ability of THF1 to either the GDP- or GTP-bound form of GPA1 (Figure 2B), whereas GST alone was not able to coprecipitate GPA1. To test whether GPA1 interacts with THF1 in vivo, we transiently expressed a full-length C-myc–tagged THF1 clone in *Arabidopsis* suspension cells (Figure 2D). Total protein was extracted with buffer containing either GDP or GTPγS and then immunoprecipitated with anti-GPA1 serum. The GPA1 preimmune serum was unable to coprecipitate THF1. Samples were subjected to immunoblotting using anti-GPA1 or anti-myc serum. As shown in Figure 2D, GPA1 and THF1-myc interacted equally well both in vitro and in vivo in the presence of either GDP or GTPγS.

Ubiquitously Expressed THF1 Is Localized to Plastids and Plastid Stromules

Our initial report on *THF1* described how its global gene expression could be regulated by light (Wang et al., 2004). Here, we show that it is expressed ubiquitously in all organs (Figure 3A), with the highest levels of *THF1* promoter:*uidA* (GUS) expression observed in roots of both light-grown (Figure 3B) and dark-grown (Figure 3C) seedlings, showing that the gene is well expressed

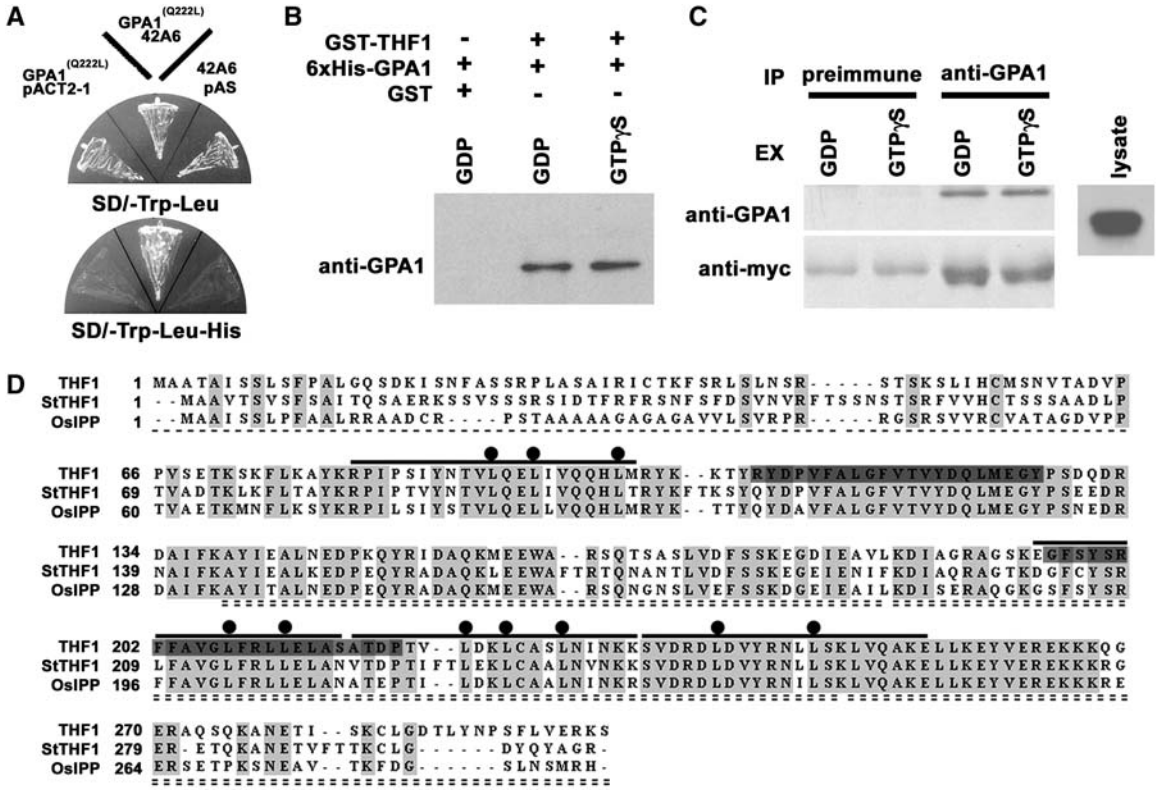

Figure 2. Interaction between GPA1 and THF1.

(A) Isolation of THF1 as a GPA1$^{(Q222L)}$-interacting protein in a yeast two-hybrid screen. GPA1$^{(Q222L)}$ is a GTPase-deficient form of GPA1. The triple-dropout plate indicates interaction between GPA1$^{(Q222L)}$ and prey 42A6 on the SD/−Leu/−Trp/−His plate. 42A6 is a partial clone corresponding to *THF1*.

(B) Both GDP- and GTPγS-bound forms of GPA1 interacted with THF1 in vitro. Purified 6xHis-GPA1 and full-length GST-THF1 were incubated in buffer with either GDP or GTPγS for 1 h, then precipitated with glutathione-agarose beads. The precipitates were probed with anti-GPA1 serum. GST alone did not bind to GPA1.

(C) Alignment of the coding sequences of THF1 homologues in higher plants using the Clustal method (BioEdit). Identical residues are highlighted in light gray, and dark gray denotes the two putative transmembrane domains (see Figure 4). Boldface lines above the sequences represent the matrix repeat sequences. Dots associated with the matrix repeats mark repeated Leu residues. The single dashed line shows the putative transit peptide. The C-terminal sequence indicated by the double dashed line was the identified prey protein from clone 42A6.

(D) GPA1 interaction with THF1 in vivo. Myc-tagged THF1 was expressed in *Arabidopsis* suspension cells and immunoprecipitated (IP) with preimmune or anti-GPA1 serum in the presence of GDP or GTPγS. The precipitates were probed with GPA1 or anti-myc antiserum.

in roots regardless of light conditions. The highest *THF1* promoter:*uidA* expression was observed in the root apical meristems (Figure 3D), similar to that observed for both *GPA1* and *RGS1* (Ullah et al., 2001; Chen et al., 2003). Immunoblot analysis of THF1 protein levels showed that the highest levels of THF1 protein were in hypocotyls (Figure 3A). The comparison between the immunoblot and GUS data suggests either a rapid turnover of THF1 protein or some form of posttranslational regulation in the root.

Confocal imaging of a 35S-driven THF1–green fluorescent protein (GFP) fusion protein in 5-d-old seedlings (Figures 3E to 3G) confirmed the earlier observation that THF1 is a plastid protein (Wang et al., 2004) but further demonstrated that THF1-GFP is present in root plastid stromules. Stromules are tubular extensions of plastids, enclosed by both the inner and outer plastid envelope (Gray et al., 2001), which are thought to increase the surface area of plastid membranes for an as yet undetermined function. It is important to note that the THF1-GFP–labeled stromules were most easily visualized in root tissues (Figures 3E and 3G), whereas none were found in leaf tissues. Time-lapse imaging of THF1-GFP in root epidermal cells and root hairs (Figure 3F; see Supplemental Movie 1 online) revealed the plastid compartments and stromules to be highly dynamic within cells, suggesting that the plastids may use their stromule extensions to interact and anchor to the plasma membrane (Figures 3E and 3G, red arrows). Tethering is a previously reported feature of stromules (Kwok and Hanson, 2004a) that may allow plastids to remain in proximity to cellular structures against the currents of cytoplasmic streaming (Gunning, 2005; Natesan et al., 2005).

THF1 Localizes to Both the Outer Plastid Membrane and the Stroma

The data presented above describe a root plastidic interaction partner to a plasma membrane–delimited G-protein. Although

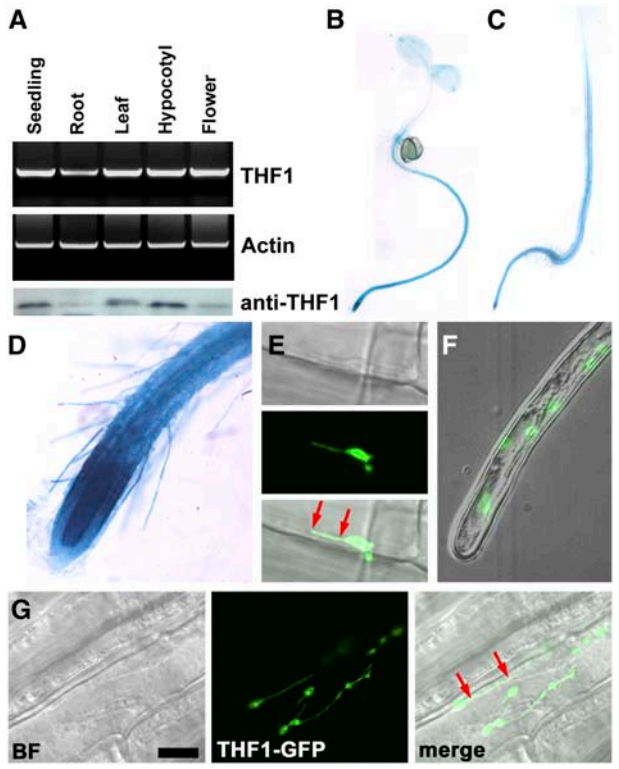

Figure 3. Tissue Expression and Subcellular Localization of THF1.

(A) *THF1* transcript and THF1 protein in different organs. Top, RT-PCR using RNA isolated from the indicated organs from 30-d-old light-grown plants and 10-d-old seedlings. Bottom, the same set of samples was used for immunoblot analysis probed with anti-THF1 serum (α-THF1). The lowest and highest signals were in the linear range of this assay.
(B) and **(C)** Transcriptional fusions between the *THF1* promoter and the *uidA* gene encoding GUS were used to transform *Arabidopsis*. Seedlings were stained for GUS activity in 5-d-old seedlings grown either in constant light **(B)** or in darkness **(C)**. Staining was stopped after 5 h to highlight the predominant expression locations, but overnight staining indicated ubiquitous expression.
(D) Root tip cells including hairs express *THF1*; the strongest expression was seen in the root meristem.
(E) to **(G)** A 35S-driven THF1-GFP fusion protein localizes to plastids and can be seen in plastid stromules that appear to tether the plastid to the plasma membrane (red arrows; see also Supplemental Movie 1 online). **(E)** and **(G)** show root epidermal cells; **(F)** shows a root hair cell. BF, bright field. Bar in **(G)** = 10 μm.

the highly vacuolated nature of root cells means that plastids and other organelles are frequently pressed up against the plasma membrane, the concept that a specific protein–protein interaction was occurring prompted us to look in more detail at the physical possibility of this unusual situation. Kyte–Doolittle hydropathy analysis of full-length THF1 using the TOPRED algorithm (von Heijne, 1992; Claros and von Heijne, 1994) set to identify prokaryotic/plastidic proteins strongly predicts the presence of at least one and possibly two membrane-spanning domains, as shown by hydrophobicity values exceeding the upper (UC) and lower (LC) cutoff values (Figure 4A). This prediction is in contrast with that extracted from the Cornell Plastid Proteome Database (Friso et al., 2004), which suggests that THF1 does not posses membrane-spanning domains. However, this discrepancy is attributable to the different prediction algorithms used to determine the presence of eukaryotic membrane-spanning domains. Further analysis of these putative transmembrane domains revealed that both their presence and sequence are highly conserved among the highly divergent taxa that contain orthologs to THF1, including rice and potato (Figure 2C). We previously showed that THF1 contains a cleaved transit peptide that facilitates entry into the plastid (Wang et al., 2004), leading us to propose two possible topology models for the remaining 239 amino acids of the mature protein within the outer plastid membrane (Figure 4B).

Both models allow for the THF1–GPA1 interaction on the external face of the plastid, consistent with our identification of the THF1-interaction region within the C-terminal 162 amino acids of the mature THF1 protein (denoted the GPA1 interaction region in Figure 4A). To confirm this in silico analysis, immunoblot analysis of fractionated plastids was performed. Intriguingly, as shown in Figure 4C, THF1 is enriched in both the outer membrane and stromal fractions. Although this is consistent with an outer membrane–spanning prediction for THF1 (Figure 4A), we applied our model for the THF1–GPA1 interaction only to the pool of THF1 that spans the outer membrane, as opposed to the stromal pool. The fact that a second pool of THF1 is found in the stromal fraction may suggest either multiple functions for THF1 in plastids or some requirement for the trafficking of THF1. Dual localization of THF1 in the fractionation data would also be consistent with a single localization in different plastid types. Although there are no known plastid-specific differences in the protein import machinery, this possibility should not be ruled out. Nonetheless, both modeling and biochemical fractionation of plastid membranes are consistent with our hypothesis of an outer membrane localization for THF1 on root plastids.

In Vivo Dynamics of the GPA1–THF1 Interaction

Förster resonance energy transfer (FRET) analysis between 35S-driven *GPA1-CFP* (for cyan fluorescent protein) and *THF1-YFP* (for yellow fluorescent protein) constructs in the *gpa1-4 thf1-1* background provided spatial resolution of the GPA1–THF1 interaction in root epidermal cells. Two-filter channel FRET analysis confirmed our earlier observations that THF1 is plastidic (Figure 5A) and GPA1 is localized to the plasma membrane (Figure 5B). We observed that the ratio of YFP to CFP was high where a plastid was adjacent to the plasma membrane. The observed FRET signal, denoted nF/I (Figure 5), corresponds to the observed YFP-CFP ratio and represents an algorithmic output for two-filter channel FRET based on the equations of Gordon et al. (1998). Simply put, it is a mathematical representation of the YFP:CFP ratio, normalized to the donor intensity. FRET requires that the donor and receiver reside within 10 to 100 Å, strongly suggesting a physical interaction between GPA1 and THF1. FRET was never observed where root plastids did not abut the plasma membrane, consistent with our demonstration that a direct physical interaction between GPA1 and THF1 occurs in vivo. Additionally, the detection of FRET between GPA1 and THF1 is consistent with an outer membrane localization for the pool of THF1 relevant to G-protein signaling, as FRET cannot

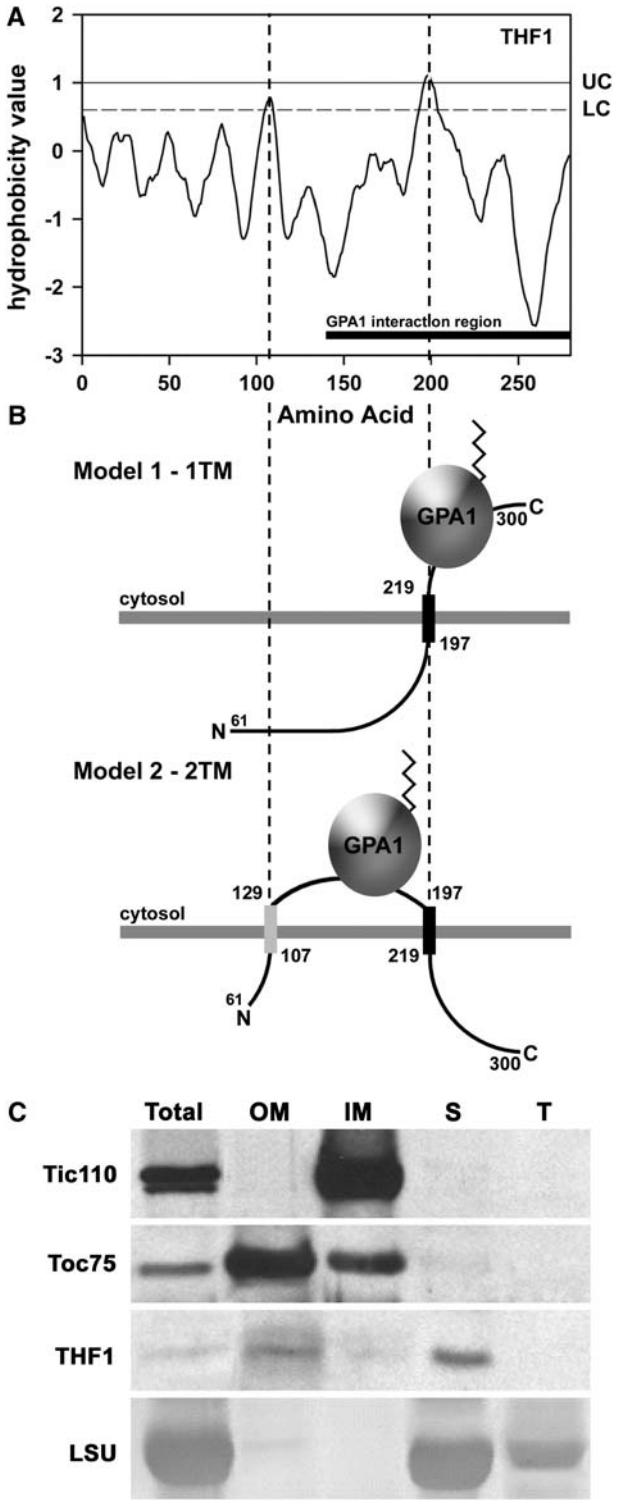

Figure 4. THF1 Is a Protein of the Outer Plastid Membrane and Stroma.

(A) Kyte–Doolittle hydropathy plot for THF1. UC and LC denote the upper and lower cutoffs for the prediction of membrane-spanning domains, respectively. The solid bar at bottom denotes the positions mapped by the yeast two-hybrid assay as the THF1–GPA1 interaction domain. Dashed lines denote positions of the two predicted membrane spans.

occur between two sequestered fluorophores, one on the plasma membrane and one on the plastid stroma, because of the extreme proximity required for energy transfer.

Although nF/I is a robust method to measure FRET, we further validated the observed FRET signal using an acceptor photobleaching method. This method is routinely used to confirm FRET between various fluorophore pairs (Bastiaens and Jovin, 1996; Bastiaens et al., 1996; Kenworthy, 2001; Vermeer et al., 2004). Its principle is that energy transfer is reduced or abolished when the acceptor fluorophore (in this case YFP) is photobleached, accompanied by dequenching of donor (CFP) fluorescence. This is a stringent diagnostic test for FRET, as in most circumstances fluorescence normally decreases after acceptor photobleaching (Karpova et al., 2003). After a 5-min irradiation at 480 nm, we found that CFP emission was dequenched in the same region where FRET was originally recorded (Figure 5H). A quantitative analysis of the nF/I recording is shown in Figure 5I. Before YFP photobleaching, the nF/I stabilized within 3 min (top gray line). After acceptor photobleaching, the FRET efficiency was reduced irreversibly to zero (bottom gray line).

thf1-1 Root Growth Is Hypersensitive to Increased D-Glucose

Our previous report described the phenotype of an insertion mutant in *THF1*. We demonstrated that a homozygous SALK insertion line (094925) is transcript null for *THF1* and that the *THF1* cDNA was capable of complementing the mutation (Wang et al., 2004). We found that the gene was necessary for correct development of the thylakoid membrane and that the null allele conferred altered plant morphology, specifically stunted growth and variegated leaves (Wang et al., 2004). To examine whether THF1 had any role in the G-protein–coupled sugar pathway, we tested the effect of increased D-glucose on the rate of *thf1-1* primary root growth (Figure 6B). Additionally, although *THF1* expression was observed in root hairs (Figure 3D), no obvious root hair phenotype was observed for this mutant (data not shown).

As shown previously, on 1% D-glucose, *gpa1-4* roots were similar to wild-type roots, although *thf1-1* roots were ~25% shorter and *thf1-1* cotyledons were pale green (Figure 6B). However, on 6% D-glucose, *thf1-1* seedlings were ~50% shorter

(B) Possible topologies for THF1 that enable interaction between the membrane-spanning pool of THF1 and the plasma membrane–delimited GPA1. THF1 contains at least one (model 1), and possibly two (model 2), membrane-spanning domains, which embed THF1 in plastid membranes. The angled line on GPA1 represents the N-terminal myristoyl group that anchors GPA1 to the plasma membrane (data not shown).

(C) Isolated plastids were fractionated and subjected to immunoblot analysis with the corresponding antisera to the indicated marker proteins or THF1. Fractions are represented as follows: Total, whole preparation; OM, outer plastid membrane; IM, inner plastid membrane; S, stromal fraction; T, thylakoid fraction. Controls used to determine THF1 localization were as follows: Tic110, a component of the inner plastid membrane; Toc75, a component of the outer plastid membrane; and the large subunit of ribulose-1,5-bisphosphate carboxylase/oxygenase (LSU), which is found in the stroma and thylakoid.

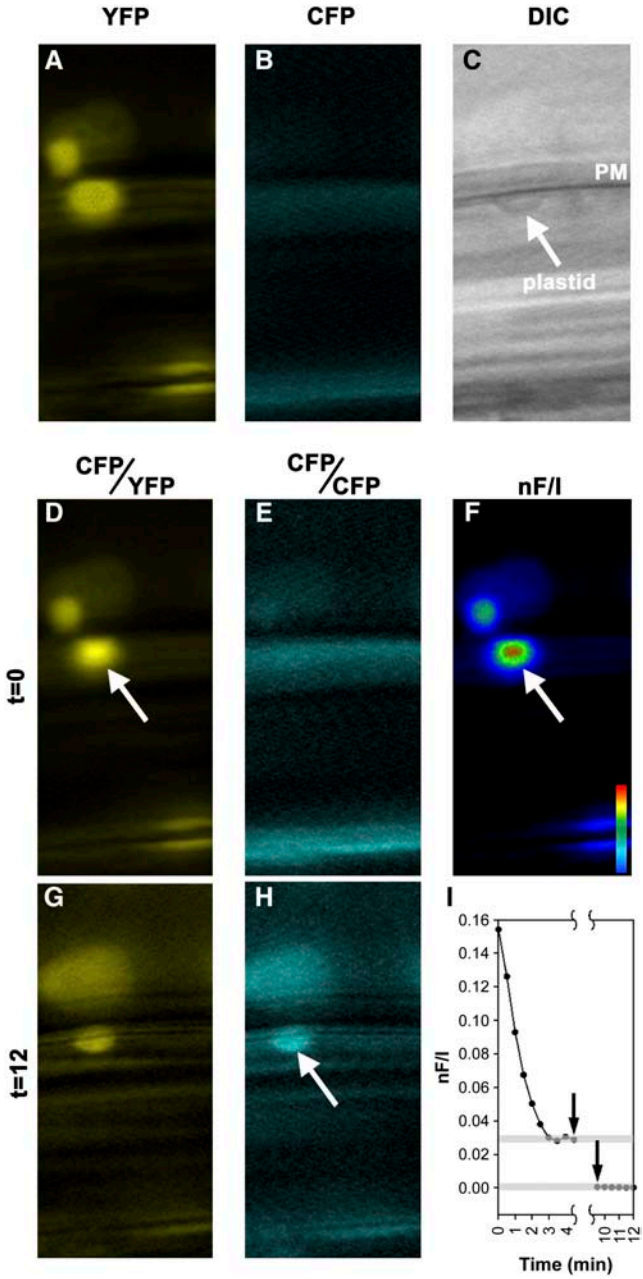

Figure 5. FRET Analysis of the GPA1–THF1 Interaction.

FRET between GPA1-CFP and THF1-YFP was calculated using established algorithms for two-filter FRET with fluorescence microscopy.
(A) to **(C)** Single images of cells expressing THF1-YFP **(A)** and GPA1-CFP **(B)** and a corresponding differential interference contrast (DIC) image **(C)**, showing plasma membrane (PM) and a plastid.
(D) to **(H)** FRET images were recorded before (**[D]** to **[F]**) and after (**[G]** and **[H]**) acceptor photobleaching. Arrows denote the localization of the observed FRET signal where a plastid abutted the plasma membrane (**[D]** and **[F]**) and the region of CFP dequenching after YFP photobleaching **(H)**.
(I) Quantification of the observed FRET signals. The first arrow denotes the start of the 480-nm irradiation, and the second arrow indicates the end.

than *gpa1-4* seedlings. Because root length is a complex trait, one that can be a result of altered germination rates, we quantitated the growth rate of the primary roots over time. On 1% D-glucose, the *thf1-1* root growth rate was ~10% lower than the wild-type rate (statistically insignificant) (Figure 6C, top); however, *thf1-1* roots were never able to recover from the growth-arresting effect of high D-glucose compared with wild-type roots (Figure 6C, bottom). This finding suggests that the loss of THF1 confers either increased sensitivity to, or the inability to adapt to, high D-glucose. To complement these data, the effects of *THF1* overexpression were tested. Two independent *THF1* overexpression lines were germinated on 1% and 6% D-glucose. Contrary to the loss of *THF1*, ectopic overexpression of *THF1* caused roots to

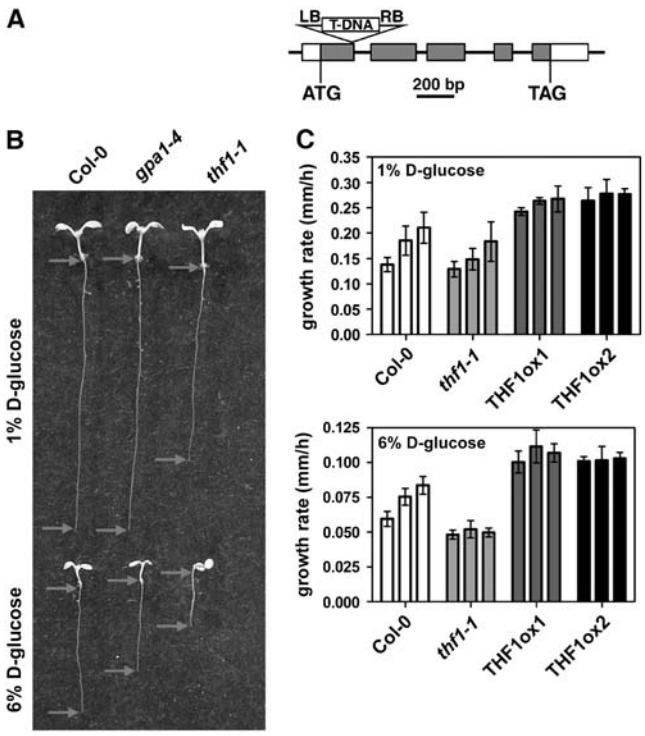

Figure 6. *THF1* Is Involved in D-Glucose Signaling.

(A) Scheme of the T-DNA insertion (SALK line 094925) in *THF1*, as described previously (Wang et al., 2004). LB, left border; RB, right border.
(B) Seedlings of Columbia, *gpa1-4*, and *thf1-1*germinated on both 1% and 6% D-glucose, showing the sensitivity of the *thf1-1* mutant to increased D-glucose compared with both the wild type and *gpa1-4*. Images show randomly selected seedlings taken from the pool used for the determination of growth rate. Arrows mark the shoot/root transition and the root tip. The growth rate of roots on increased D-glucose is reduced in *thf1-1* seedlings.
(C) Tolerance to high levels of D-glucose can be conferred by overexpression of *THF1*. The rate of growth of the primary root was assayed over a 3-d period (each set of three bars), beginning 48 h after exposure to light. The interval rate is expressed as millimeters of growth per hour, averaged over each 24-h period. Error bars represent SE. $n > 10$. THF1ox, ectopically overexpressed *THF1*.

grow at faster rates on either low or high D-glucose compared with the wild type at all times.

This difference in phenotypes between *gpa1-4* and *thf1-1* enabled epistasis analysis between the *gpa1-4* and *thf1-1* alleles. The double mutant exhibited the same root-development phenotype as the *thf1-1* null mutant on both normal and increased levels of D-glucose (see Supplemental Figure 1 online). This finding suggests a relationship between the two genes, which is consistent with our hypothesis that THF1 operates downstream of GPA1 in the G-protein–coupled sugar-signaling pathway.

THF1 Protein Levels Are Affected by D-Glucose

To test a mechanistic role for THF1 in sugar signaling, we quantitated the effect of D-glucose on the steady state level of THF1 protein by imaging and immunoblot analysis (Figure 7). As shown previously, *35S*:*THF1-GFP* fluorescence was observed in plastids through the roots of 5-d-old seedlings (Figures 3E to 3G), including the root meristem. However, after 30 min of 6% D-glucose treatment, observable GFP fluorescence in roots was diminished. The four panels of Figure 7A are conventional fluorescence microscopy images of the same root and are representative of >20 roots assayed. No decrease in the levels of *35S*:*THF1-GFP* fluorescence was observed after treatment with L-glucose (Figure 7A), NaCl, or mannitol. Sugar-induced changes in THF1-GFP fluorescence were not observed in the leaves.

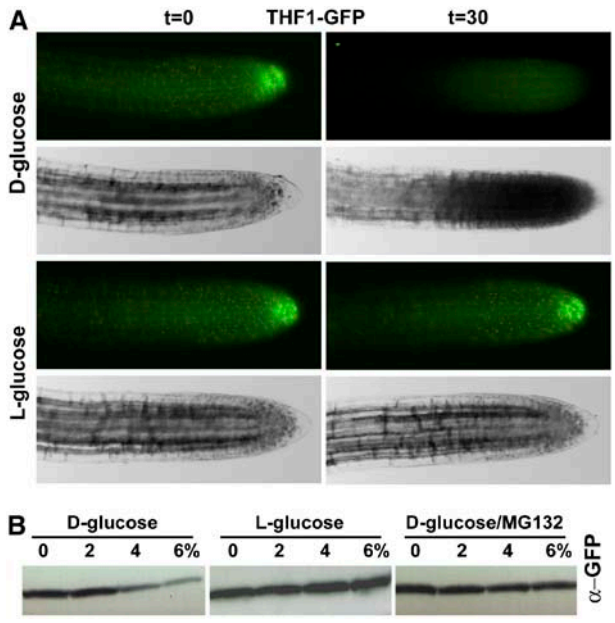

Figure 7. D-Glucose Has a Direct Effect on THF1 Steady State Level.

(A) Green fluorescence in root cells expressing a 35S-driven THF1-GFP fusion protein disappeared 30 min after being treated with 6% D-glucose, but not L-glucose

(B) THF1-GFP degradation at the indicated applied glucose levels (%) for 30 min was confirmed by immunoblotting probed with anti-GFP antiserum. Degradation did not occur with L-glucose treatment and was inhibited by the general protease inhibitor MG132. Not shown are nontransformed roots, which did not display fluorescence under these excitation and digital capture conditions.

Immunoblot analysis was used to confirm that the observed loss of signal was specific to D-glucose and that it was attributable to protein degradation (Figure 7B). Protein samples from *35S*:*THF1-GFP* seedlings were extracted from seedlings treated with 0, 2, 4, or 6% D-glucose for 30 min and subjected to SDS-PAGE and immunoblot analysis with anti-GFP antibodies. As seen in Figure 7B, the steady state level of THF1-GFP protein was reduced over 30 min in a dose-dependent manner. However, in samples treated with L-glucose, the steady state level of THF1-GFP remained constant, showing specificity for the D-stereoisomer. Samples treated with D-glucose in the presence of the protease inhibitor MG132 did not show changes over time in THF1 steady state levels, suggesting that THF1 half-life is influenced by high D-glucose levels.

DISCUSSION

THF1 Is an Interaction Partner for Gα in the Sugar-Signaling Pathway in Roots

Six lines of evidence indicate that THF1, a plastid protein, interacts with the plasma membrane–delimited G-protein, GPA1, and four lines of evidence indicate that THF1 has a role in sugar signaling.

The GPA1–THF1 interaction is demonstrated by the following findings. (1) In a yeast two-hybrid conformation, the C-terminal 162 residues of THF1 interact with the constitutively active form of GPA1. (2) This interaction in yeast was confirmed in vitro using recombinant full-length THF1 and GPA1. (3) In vivo interaction in plant cells was shown through coimmunoprecipitation of GPA1 with THF1. (4) Genetic epistasis analysis between the loss-of-function alleles *gpa1-4* and *thf1-1* is consistent with the two corresponding gene products operating in the same pathway. (5) THF1 is at least in part localized to the outer membrane of plastid stromules, which appear to associate with the plasma membrane. (6) FRET analysis between fluorophore-tagged GPA1 and THF1 confirms the interaction in vivo and provides spatial information.

The evidence that THF1 has a direct or indirect role in sugar signaling is based on both biochemical and genetic experiments. (1) *thf1-1* loss-of-function mutants are hypersensitive to and unable to recover from exogenous D-glucose. (2) *THF1*-overexpressing plants have a higher rate of root growth on high D-glucose. (3) An epistatic relationship between the *thf1-1* and *gpa1-4* alleles places *THF1* genetically on the G-protein–coupled sugar-signaling pathway. (4) Exogenous D-glucose, but not L-glucose, causes a rapid degradation of THF1 protein.

THF1 was shown to interact similarly with either the GDP- or GTP-bound form of GPA1 (Figure 2). THF1 may be a component of the heterotrimeric complex but does not preferentially interact with the activated form of the Gα subunit, suggesting a scaffolding or tethering role for THF1, perhaps to maximize signaling between the plasma membrane and plastids in response to D-glucose. This possibility implies that the primary function of THF1 is not signaling per se but to act as a maintenance or accessory protein. However, as in vitro and in vivo interaction

shown by in vitro and in vivo coimmunoprecipitation is based on end-point analysis rather than kinetics, we do not exclude the possibility that THF1 affinity for GPA1 is affected by the GDP/GTP state and is not detected in our assay. Modeling based on data from kinetic analyses may reveal small affinity differences that have a large impact on the ratio of the GTP- and GDP-bound states as they are allosterically amplified through the coupled effector interactions, as is the case for human Gα subunits (Hatley et al., 2003). Detailed kinetics analyses are also needed to determine whether THF1 has GAP activity on $GPA1^{GTP}$. Because the designation of THF1 as a Gα effector awaits evidence for either a demonstrated GAP activity or different binding affinities for the two nucleotide states of GPA1, other roles, such as structural or targeting, should not be ruled out.

It should be noted that it is likely that THF1 acts in pathways other than those coupled by the heterotrimeric G-protein, for three reasons. (1) The expression pattern of *THF1* (Figure 3) extends outside the limited areas of *GPA1*. (2) The loss-of-function phenotypes of *thf1-1* mutants are pleiotropic, beyond the narrowly defined traits of the *gpa1* mutant. (3) Plastid fractionation data showed that THF1 was localized to both the outer plastid membrane and the stroma, suggesting that THF1 may perform an additional role in the stroma, where GPA1 should be excluded. Although the dual localization of plastid proteins is unusual, it is not unique to THF1, as other plastid proteins have dual localization and function (Tu et al., 1999). Thus, it should be considered that although GPA1 can be a regulator of THF1, it might not be the only one. Also, on this point, we do not exclude exclusive locations for THF1 of either the outer membrane or the stroma but in different pools of plastids, because our fractionation data do not distinguish between potentially different plastid types.

The initial observations of *thf1-1*, showing that it lacked properly formed thylakoid membranes, are consistent with a structural or trafficking role (Wang et al., 2004). Indeed, it could be the case that the phenotypes pertaining to improper thylakoid formation may relate to the lack of the stromal pool of THF1, whereas the D-glucose–sensitive phenotypes are related to a lack of the THF1–GPA1 interaction. If this interaction functions to either mediate or transduce signals between the plasma membrane and the plastids, a lack of this interaction may represent an aberration in the ability of root plastids to regulate such processes as starch synthesis.

Despite the broad expression pattern of THF1, the highest levels observed with the *THF1* promoter:GUS fusion were in the root meristem, correlating with strong expression of *GPA1* (Ullah et al., 2001). As *thf1-1* meristems have normal histology and gravitropic responses (data not shown), this disfavors a developmental defect as the cause for the observed seedling hypersensitivity to D-glucose.

THF1 Mediates Signaling between the Plasma Membrane and the Plastids

How THF1, a plastid protein, is able to interact with the plasma membrane–delimited GPA1 is an intriguing question. Plastids are well known for their dynamic shape change and movement, but the diversity of plastids based on their function is essentially unknown beyond the classic three plastid types: chloroplasts, leukoplasts, and amyloplasts. Plastids can migrate freely in the cytoplasm or adhere to the plasma membrane through actin cages, depending on different cell types and growth conditions (Kwok and Hanson, 2004c; Gunning, 2005). The discovery of stromules, tube-like extensions of the plastid envelope and stroma, revealed a unique mechanism by which plastid molecules can communicate with other cell compartments and indeed other plastids (Kwok and Hanson, 2004a, 2004d). Others have reported that stromules are able to form bead-like structures that move around the cell as part of a stromule network or even as free vesicles (Pyke and Howells, 2002; Natesan et al., 2005). Such plastid-derived vesicles are highly reminiscent of vesicles trafficking along a filamentous network. Evidence for plastid communication with other subcellular compartments is scant but increasing (Chew et al., 2003; Strand et al., 2003). The observed FRET between GPA1 and THF1 indicates that the interaction occurs at the interface between the plastid and the plasma membrane, and because the interaction was monitored over several minutes (to allow for acceptor photobleaching), this may suggest that plastids that interact with the plasma membrane do not move as freely within the cytosol as untethered plastids. Our time-lapse acquisition of stromule movement in roots is consistent with this finding (see Supplemental Movie 1 online).

The prediction of membrane-spanning domains in THF1 and the identification of an outer membrane–localized pool of THF1 render the four interaction data sets interpretable and suggest a direct link between plastids and the plasma membrane. Of the two topological models proposed in Figure 4B, model 1 is the most likely because it fits the THF1-GFP degradation data shown in Figure 7E: in this model, the C terminus of THF1 is fully exposed to the cytosol for potential ubiquitination and subsequent degradation (Vierstra, 2003). However, although the inhibitor MG132 is typically associated with inhibition of the function of the cytosolic 26S proteasome (Yang et al., 2004), and considering that THF1 is both a plastidic and/or a membrane-spanning protein, we cannot rule out the possibility that the MG132 acts as an inhibitor of a protease not operating in the 26S proteasome pathway. Another possibility is that an as yet unidentified MG132-sensitive degradation machinery is present in plastids, which could be responsible for the degradation of both the membrane and soluble pools of THF1.

We expect that plant cells precisely coordinate biosynthetic activities with the export of molecules from plastids to their destinations in response to internal and external signals (Eastmond and Graham, 2003; Tiessen et al., 2003; Kolbe et al., 2005). Consideration of known vesicular trafficking mechanisms is a particularly suitable approach to such an issue, because trafficking machineries are highly conserved in eukaryotes and are responsible for delivering and recycling many kinds of molecules, including protein and lipid components of the membrane, to various compartments (Maxfield and McGraw, 2004). For example, in pancreatic β-cells, heterotrimeric G-proteins are important molecular switches that control insulin secretion via endocytosis and exocytosis to ensure the vital function of glucose homeostasis (Konrad et al., 1995; Lang, 1999; Skoglund et al., 1999; Luo et al., 2001). The colocalization of GPA1 and its physical interactor, THF1, at the plasma membrane suggests that plastid molecules such as THF1 communicate with plasma membrane–delimited molecules via two

possible mechanisms. One possibility is to produce a lipid microdomain that can serve as a platform to assemble G-protein complexes at the plasma membrane. THF1 may establish the specificity of the G-protein signaling pathway or the regulation of receptor-mediated endocytosis in a GPA1-dependent manner. The second possibility is that THF1 together with GPA1 plays a role in exocytosis at stromule–plasma membrane sites.

Heterotrimeric G-Protein–Coupled Sugar Signaling

All of the data presented here and elsewhere are consistent with the prevailing notion that D-glucose acts as a hormone-like signal, although a physiological concentration range of extracellular D-glucose in signaling has yet to be defined. High applications of D-glucose (Arenas-Huertero et al., 2000) cause physiologically appropriate responses, and genetic screens for mutants resistant to high D-glucose have revealed known elements in sugar signaling (Xiao et al., 2000; Moore et al., 2003). Because cells develop in a wide range of D-glucose concentrations, a sugar-signaling mechanism operating from presumably 30 to 300 mM or higher D-glucose is expected. Molar levels of D-glucose are found in tissues such as fruit, but the levels of extracellular D-glucose in vegetative tissues such as root have yet to be successfully evaluated. Indirect measurements have been applied to address this problem, and estimates of apoplastic levels of D-glucose at 150 mM (3%) or higher have been proposed (McLaughlin and Boyer, 2004; Makela et al., 2005). For example, sorghum (*Sorghum bicolor*) embryos develop in as high as 6% apoplastic D-glucose (Maness and Mcbee, 1986).

What is the nature and mechanism of the high-glucose-induced root growth arrest? Little is known about how sugars control growth and development in plants. We found that root cells grown on high D-glucose become severely expanded (data not shown), suggesting a possible control of the cell division/expansion pathway. This is entirely consistent with the now firmly established role of the G-protein complex in the modulation of cell division (Ullah et al., 2001, 2003; Chen et al., 2003; Jones et al., 2004). Sugars control cyclin D expression in plant cells (Riou-Khamlichi et al., 2000), and a loss-of-function mutation in a moss cyclin D gene caused a D-glucose–resistant phenotype (Lorenz et al., 2003). In addition, sugars control the G1-to-S phase transition (Menges and Murray, 2002). Thus, it is becoming clear that sugars act as signals to modulate plant cell proliferation and do so by a complex set of signaling mechanisms. Hexokinase is needed for intracellular glucose detection, and now, with the introduction of both THF1 and RGS1 (Chen et al., 2003; Chen and Jones, 2004), a signaling network involving a heterotrimeric G-protein is added to our understanding of D-glucose signaling in *Arabidopsis*. Because these organelles either use or produce D-glucose or its catabolites, it is reasonable to assume that extracellular glucose availability would influence cellular glucose economy potentially as it occurs in yeast.

METHODS

Plant Growth Conditions, Plasmid Construction, Antiserum, and Transformation

The *Arabidopsis thaliana* ecotype used in this study was Columbia with the exception of the GPA1-overexpressing lines (Figure 1B), which were in Ws. Seeds were surface-sterilized and stratified for 4 to 5 d before germination at 22°C on half-strength Murashige and Skoog medium containing the indicated concentrations of D-glucose. Plants were grown under short-day conditions. Where required, plates were scored for root length daily and the data analyzed using ImageJ. All whole-seedling images were taken with a Sony DSC-F717 digital camera.

The various plasmids were constructed using the Gateway cloning system (Invitrogen). For clarity in gene, mutant, and protein designations, the gene corresponding to the locus of At2g20890 is referred to as *THF1*, its open reading frame is referred to as *THF1*, the null mutant is referred to as *thf1-1*, and the protein is referred to as THF1. *THF1* was inserted into the entry vector pENTR/D-TOPO (Invitrogen) by topoisomerase-mediated ligation and then recombined into destination vectors pDEST15, pDEST24 (Invitrogen), pGWB5 (35S-driven C-terminal GFP fusion), pGWB6 (35S-driven overexpression), and pGWB41 (35S-driven C-terminal YFP fusion) (Research Institute of Molecular Genetics) to create the various expression vectors for *Escherichia coli* and plants. The GTPase-deficient form of GPA1$^{(Q222L)}$ is described by Chen et al. (2003). *Arabidopsis* plants were transformed by the flower-dip method (Bechtold et al., 1993). Transgenic T1 plants were identified by kanamycin resistance.

Antiserum to THF1 was raised in rabbits (Cocalico Biologicals) as described previously (Wang et al., 2004). Antisera to GPA1 (9271 and 9272) were generated in rabbits using as antigen the C-terminal peptide of GPA1 (DETLRRRNLLEAGLL) coupled to keyhole limpet hemocyanin via an N-terminal Cys thioester linkage.

Identification and Analysis of Mutants and Transgenic Plants

The homozygous T-DNA insertion mutant *thf1-1* was generated from the Salk Institute sequence-indexed insertion mutant collection (http://signal.salk.edu/smission.html) as described previously (Wang et al., 2004). The *THF1* transcript level was quantified using the ThermoScript RT-PCR system (Invitrogen) together with gene-specific primers and THF1 protein levels by immunoblot analysis with the anti-THF1 polyclonal antibody. The *gpa1-4 thf1-1* double mutant was generated by genetic crosses, and homozygous lines were identified by genotyping and confirmed by PCR-based genotyping. The GPA1-CFP and THF1-YFP single transformants were generated by the floral-dipping method from *gpa1-4* and *thf1-1* plants, respectively, and screened by fluorescence microscopy and RT-PCR. GPA1-CFP and THF1-YFP double-transgene plants were created by genetic crosses of the transformed parents using lines selected to ensure that transgene expression was not higher than in the wild type. The *THF1* overexpression lines were screened by immunoblot analysis (data not shown). GUS activity in situ was performed as described by Jefferson et al. (1987).

Yeast Two-Hybrid Screens

Yeast strains were grown at 30°C in standard rich medium (yeast peptone dextrose [YPD]) or synthetic medium (synthetic dextrose [SD]) supplemented with the appropriate amino acids. Yeast two-hybrid screens were performed using an interaction mating protocol as described previously (Soellick and Uhrig, 2001). A yeast mating procedure was performed for the verification of positive clones. Gap-repair cloning was used to recombine the candidate PCR products with the linearized vector pACT2-1 in yeast strain AH109. The bait vector pAS-GPA1$^{(Q222L)}$ was transformed into Y187 strain. For mating, one colony of each type was suspended in YPD medium and incubated at 30°C for 5 h. YPD medium was removed after centrifugation, and cells were resuspended in 200 μL of water. Half of the culture was spread on SD/−Leu/−Trp plates and half on SD/−Leu/−Trp/−His/+3-aminotriazole plates. The growth of yeast was checked 48 h after plating. Growth on the corresponding single-dropout plates indicated transformation (data not shown). The cDNAs used for the prey screens were generously provided by Csaba Koncz and Hans Sommer (Max-Planck Institüt für Züchtungsforschung).

Protein Coimmunoprecipitation Assay

For in vitro protein purification and interaction, 6xHis-GPA1 and GST-THF1 fusion proteins were purified from BL21(DE3) cells using affinity chromatography according to the manufacturer's instructions (6xHis-GPA1, Clontech; GST-THF1, Amersham). Poly-His-GPA1 was loaded with GDP or GTPγS before adding GST-THF1 to test the specific binding of GPA1 to THF1 in buffer A (50 mM Tris-HCl, pH 7.5, 50 mM NaCl, 2 mM DTT, 5 mM $MgSO_4$, protease inhibitor cocktail for bacterial cell extracts [Sigma-Aldrich], and 100 μM GDP or GTPγS). The samples were incubated at 25°C for 1 h in the presence of glutathione-agarose, washed five times with the buffer, and eluted with 2× SDS-PAGE sample buffer. Proteins were separated by SDS-PAGE and immunoblotted with anti-GPA1 (rabbit polyclonal antiserum raised against a peptide representing the last 15 amino acids of GPA1, designations 9271 and 9272) and anti-GST (Sigma-Aldrich) antibodies.

For in vivo coimmunoprecipitation, the myc epitope–tagged *THF1* binary vector was transformed into *Arabidopsis* suspension cells (a gift from Csaba Koncz, Max-Planck Institüt für Züchtungsforschung) by *Agrobacterium tumefaciens*–mediated transformation. Cells were cultured and harvested as described by Ferrando et al. (2000). Total protein was extracted with buffer (as described above plus the addition of 1% Triton X-100). The expression level of the myc-THF1 fusion protein was confirmed by immunoblotting with an anti–c-myc antibody (mouse monoclonal 9E10; Santa Cruz Biotechnology) before coimmunoprecipitation was performed according to procedures described elsewhere (Booden et al., 2002). Immunoprecipitated proteins were then resolved by SDS-PAGE, transferred to HybondP polyvinylidene difluoride membranes (Amersham Biosciences), and probed with the indicated antisera and antibodies.

FRET Microscopy

Fluorescence images of GPA1-CFP and THF1-YFP seedlings were captured using an Olympus IX81 inverted microscope controlled by IPlab software version 3.6 (Scanalytics). Images of CFP, YFP, and the CFP:YFP ratio were observed through a ×60 water-immersion objective and simultaneously captured by a cooled charge-coupled device camera (Photometrics Cascade digital camera; Roper Scientific) equipped with an OI-05-EM CFP/YFP FRET emission filter in a dual-view mounting tube. Filter sets used were YFP (excitation, 500/20 nm; emission, 535/30 nm), CFP (excitation, 436/20 nm; emission, 480/40 nm), and FRET (505dcxr; excitation, 436/20 nm; emission, 480/30 and 535/40 nm). For the YFP photobleaching FRET analysis, the YFP acceptor was photobleached by a 5-min, 480-nm irradiation. Calculation of normalized net FRET (nF/I) was performed with IPlab version 3.6 software, which uses established algorithms for two-filter FRET with fluorescence microscopy (Gordon et al., 1998).

Plastid Fractionation

Plastids were isolated and fractionated as described previously (Inaba et al., 2005). Essentially, chloroplasts were isolated from 15- to 20-d-old seedlings grown on 0.5× Murashige and Skoog plates supplemented with sucrose as described previously (Smith et al., 2002). Isolated intact chloroplasts were separated into membrane and soluble fractions by lysis in 0.1 M Na_2CO_3, pH 11.5, followed by centrifugation at 200,000*g* for 20 min. The pellets (membrane fraction) were directly dissolved in SDS-PAGE sample buffer. The soluble proteins were recovered by precipitation with trichloroacetic acid and dissolved into SDS-PAGE sample buffer. Intact chloroplasts were treated with trypsin as described previously (Jackson et al., 1998).

Total protein extracts from *Arabidopsis* were obtained by directly homogenizing leaves in SDS-PAGE sample buffer, unless specified otherwise. To avoid proteolytic degradation, the extraction buffer was supplemented with 2000-fold diluted protease inhibitor cocktail for plant cell extracts (Sigma-Aldrich). Extraction of total proteins from different organs of soil-grown plants was done as described (Rensink et al., 1998).

Accession Numbers

Sequence data of the genes used in this article can be found in the GenBank/EMBL data libraries under accession numbers NM_127659 (*THF1*) and NM_128187 (*GPA1*). Arabidopsis Genome Initiative locus identifiers for the genes mentioned in this article are At2g20890 (*THF1*) and At2g26300 (*GPA1*).

Supplemental Data

The following materials are available in the online version of this article.

Supplemental Movie 1. Dynamics of Stromule Interactions with the Plasma Membrane.

Supplemental Figure 1. Epistasis Analysis between *thf1* and *gpa1* Loss-of-Function Alleles for Sugar Sensitivity.

ACKNOWLEDGMENTS

We thank Peter Devreotes and Tian Jin of Johns Hopkins University for providing YFP and CFP cDNAs and advice on FRET microscopy, and Robert Bagnell, Jing Yang, Chris Breen, KwangChul Oh, and Tony Perdue, all of the University of North Carolina at Chapel Hill, for technical assistance. We thank Xin He (University of North Carolina at Chapel Hill) for help with the FRET normalization algorithm, and Brett Tyler (Virginia Bioinformatics Institute, Virginia Polytechnic Institute and State University) for proposing to us that THF1 is an integral membrane protein and for his supporting data. Work in A.M.J.'s laboratory on the *Arabidopsis* G-protein is supported by the National Institute of General Medical Sciences (Grant GM65989-01), the National Science Foundation (Grant MCB-0209711), and the U.S. Department of Energy (Grant DE-FG02-05ER15671).

Received August 19, 2005; revised March 7, 2006; accepted March 15, 2006; published March 31, 2006.

REFERENCES

Arenas-Huertero, F., Arroyo, A., Zhou, L., Sheen, J., and Leon, P. (2000). Analysis of *Arabidopsis* glucose insensitive mutants, gin5 and gin6, reveals a central role of the plant hormone ABA in the regulation of plant vegetative development by sugar. Genes Dev. **14,** 2085–2096.

Bastiaens, P.I., and Jovin, T.M. (1996). Microspectroscopic imaging tracks the intracellular processing of a signal transduction protein: Fluorescent-labeled protein kinase C beta I. Proc. Natl. Acad. Sci. USA **93,** 8407–8412.

Bastiaens, P.I., Majoul, I.V., Verveer, P.J., Soling, H.D., and Jovin, T.M. (1996). Imaging the intracellular trafficking and state of the AB5 quaternary structure of cholera toxin. EMBO J. **15,** 4246–4253.

Bechtold, N., Ellis, J., and Pelletier, G. (1993). In planta Agrobacterium mediated gene transfer by infiltration of adult *Arabidopsis thaliana* plants. C. R. Acad. Sci. Paris **316,** 1194–1199.

Booden, M.A., Siderovski, D.P., and Der, C.J. (2002). Leukemia-associated Rho guanine nucleotide exchange factor promotes G alpha q-coupled activation of RhoA. Mol. Cell. Biol. **22,** 4053–4061.

Booker, F.L., Burkey, K.O., Overmyer, K., and Jones, A.M. (2004). Differential responses of G-protein *Arabidopsis thaliana* mutants to ozone. New Phytol. **162,** 633–641.

Chen, J.G., and Jones, A.M. (2004). AtRGS1 Function in *Arabidopsis thaliana.* Methods Enzymol. **389,** 338–350.

Chen, J.G., Willard, F.S., Huang, J., Liang, J., Chasse, S.A., Jones, A.M., and Siderovski, D.P. (2003). A seven-transmembrane RGS protein that modulates plant cell proliferation. Science **301,** 1728–1731.

Chen, Y., Ji, F., Xie, H., Liang, J., and Zhang, J. (2006). The regulator of G-protein signaling proteins involved in sugar and abscisic acid signaling in *Arabidopsis* seed germination. Plant Physiol. **140,** 302–310.

Chew, O., Rudhe, C., Glaser, E., and Whelan, J. (2003). Characterization of the targeting signal of dual-targeted pea glutathione reductase. Plant Mol. Biol. **53,** 341–356.

Claros, M.G., and von Heijne, G. (1994). TopPred II: An improved software for membrane protein structure predictions. Comput. Appl. Biosci. **10,** 685–686.

Colombo, S., Ma, P., Cauwenberg, L., Winderickx, J., Crauwels, M., Teunissen, A., Nauwelaers, D., de Winde, J.H., Gorwa, M.F., Colavizza, D., and Thevelein, J.M. (1998). Involvement of distinct G-proteins, Gpa2 and Ras, in glucose- and intracellular acidification-induced cAMP signalling in the yeast *Saccharomyces cerevisiae.* EMBO J. **17,** 3326–3341.

Devoto, A., Piffanelli, P., Nilsson, I., Wallin, E., Panstruga, R., von Heijne, G., and Schulze-Lefert, P. (1999). Topology, subcellular localization, and sequence diversity of the Mlo family in plants. J. Biol. Chem. **274,** 34993–35004.

Eastmond, P.J., and Graham, I.A. (2003). Trehalose metabolism: A regulatory role for trehalose-6-phosphate? Curr. Opin. Plant Biol. **6,** 231–235.

Ferrando, A., Farras, R., Jasik, J., Schell, J., and Koncz, C. (2000). Intron-tagged epitope: A tool for facile detection and purification of proteins expressed in Agrobacterium-transformed plant cells. Plant J. **22,** 553–560.

Fischetti, V.A. (1989). Streptococcal M protein: Molecular design and biological behavior. Clin. Microbiol. Rev. **2,** 285–314.

Friso, G., Giacomelli, L., Ytterberg, A.J., Peltier, J.B., Rudella, A., Sun, Q., and Wijk, K.J. (2004). In-depth analysis of the thylakoid membrane proteome of *Arabidopsis thaliana* chloroplasts: New proteins, new functions, and a plastid proteome database. Plant Cell **16,** 478–499.

Gordon, G.W., Berry, G., Liang, X.H., Levine, B., and Herman, B. (1998). Quantitative fluorescence resonance energy transfer measurements using fluorescence microscopy. Biophys. J. **74,** 2702–2713.

Gray, J.C., Sullivan, J.A., Hibberd, J.M., and Hansen, M.R. (2001). Stromules: Mobile protrusions and interconnections between plastids. Plant Biol. **3,** 223–233.

Gunning, B.E.S. (2005). Plastid stromules: Video microscopy of their outgrowth, retraction, tensioning, anchoring, branching, bridging, and tip-shedding. Protoplasma **225,** 33–42.

Hatley, M.E., Lockless, S.W., Gibson, S.K., Gilman, A.G., and Ranganathan, R. (2003). Allosteric determinants in guanine nucleotide-binding proteins. Proc. Natl. Acad. Sci. USA **100,** 14445–14450.

Herwald, H., Cramer, H., Morgelin, M., Russell, W., Sollenberg, U., Norrby-Teglund, A., Flodgaard, H., Lindbom, L., and Bjorck, L. (2004). M protein, a classical bacterial virulence determinant, forms complexes with fibrinogen that induce vascular leakage. Cell **116,** 367–379.

Inaba, T., Alvarez-Huerta, M., Li, M., Bauer, J., Ewers, C., Kessler, F., and Schnell, D.J. (2005). *Arabidopsis* Tic110 is essential for the assembly and function of the protein import machinery of plastids. Plant Cell **17,** 1482–1496.

Jackson, D.T., Froehlich, J.E., and Keegstra, K. (1998). The hydrophilic domain of Tic110, an inner envelope membrane component of the chloroplastic protein translocation apparatus, faces the stromal compartment. J. Biol. Chem. **273,** 16583–16588.

Jang, J.C., Leon, P., Zhou, L., and Sheen, J. (1997). Hexokinase as a sugar sensor in higher plants. Plant Cell **9,** 5–19.

Jefferson, R.A., Kavanagh, T.A., and Bevan, M.W. (1987). GUS fusions: Beta-glucuronidase as a sensitive and versatile gene fusion marker in higher plants. EMBO J. **6,** 3901–3907.

Jones, A.M., and Assmann, S.M. (2004). Plants: The latest model system for G-protein research. EMBO Rep. **5,** 572–578.

Jones, A.M., Ullah, H., and Chen, J.G. (2004). Dual pathways for auxin regulation of cell division and expansion. In Tobacco BY-2 Cells, D. Inze, ed (Berlin: Springer), pp. 180–191.

Joo, J.H., Wang, S., Chen, J.G., Jones, A.M., and Fedoroff, N.V. (2005). Different signaling and cell death roles of heterotrimeric G protein alpha and beta subunits in the *Arabidopsis* oxidative stress response to ozone. Plant Cell **17,** 957–970.

Karpova, T.S., Baumann, C.T., He, L., Wu, X., Grammer, A., Lipsky, P., Hager, G.L., and McNally, J.G. (2003). Fluorescence resonance energy transfer from cyan to yellow fluorescent protein detected by acceptor photobleaching using confocal microscopy and a single laser. J. Microsc. **209,** 56–70.

Kenworthy, A.K. (2001). Imaging protein-protein interactions using fluorescence resonance energy transfer microscopy. Methods **24,** 289–296.

Kolbe, A., Tiessen, A., Schluepmann, H., Paul, M., Ulrich, S., and Geigenberger, P. (2005). Trehalose 6-phosphate regulates starch synthesis via posttranslational redox activation of ADP-glucose pyrophosphorylase. Proc. Natl. Acad. Sci. USA **102,** 11118–11123.

Konrad, R.J., Young, R.A., Record, R.D., Smith, R.M., Butkerait, P., Manning, D., Jarett, L., and Wolf, B.A. (1995). The heterotrimeric G-protein Gi is localized to the insulin secretory granules of beta-cells and is involved in insulin exocytosis. J. Biol. Chem. **270,** 12869–12876.

Kwok, E.Y., and Hanson, M.R. (2004a). Plastids and stromules interact with the nucleus and cell membrane in vascular plants. Plant Cell Rep. **23,** 188–195.

Kwok, E.Y., and Hanson, M.R. (2004b). Stromules and the dynamic nature of plastid morphology. J. Microsc. **214,** 124–137.

Kwok, E.Y., and Hanson, M.R. (2004c). In vivo analysis of interactions between GFP-labeled microfilaments and plastid stromules. BMC Plant Biol. **4,** 2.

Kwok, E.Y., and Hanson, M.R. (2004d). GFP-labelled Rubisco and aspartate aminotransferase are present in plastid stromules and traffic between plastids. J. Exp. Bot. **55,** 595–604.

Lang, J. (1999). Molecular mechanisms and regulation of insulin exocytosis as a paradigm of endocrine secretion. Eur. J. Biochem. **259,** 3–17.

Lapik, Y.R., and Kaufman, L.S. (2003). The *Arabidopsis* cupin domain protein AtPirin1 interacts with the G protein alpha-subunit GPA1 and regulates seed germination and early seedling development. Plant Cell **15,** 1578–1590.

Lemaire, K., Van de Velde, S., Van Dijck, P., and Thevelein, J.M. (2004). Glucose and sucrose act as agonist and mannose as antagonist ligands of the G protein-coupled receptor Gpr1 in the yeast *Saccharomyces cerevisiae.* Mol. Cell **16,** 293–299.

Lorenz, S., Tintelnot, S., Reski, R., and Decker, E.L. (2003). Cyclin D-knockout uncouples developmental progression from sugar availability. Plant Mol. Biol. **53,** 227–236.

Luo, X., Popov, S., Bera, A.K., Wilkie, T.M., and Muallem, S. (2001). RGS proteins provide biochemical control of agonist-evoked [Ca2+]i oscillations. Mol. Cell **7,** 651–660.

Ma, H., Yanofsky, M.F., and Meyerowitz, E.M. (1990). Molecular cloning and characterization of GPA1, a G protein alpha subunit gene from *Arabidopsis thaliana.* Proc. Natl. Acad. Sci. USA **87,** 3821–3825.

Makela, P., McLaughlin, J.E., and Boyer, J.S. (2005). Imaging and quantifying carbohydrate transport to the developing ovaries of maize. Ann. Bot. (Lond.) **96,** 939–949.

Maness, N.O., and Mcbee, G.G. (1986). Role of placental sac in endosperm carbohydrate import in sorghum caryopses. Crop Sci. **26,** 1201–1207.

Mason, M.G., and Botella, J.R. (2000). Completing the heterotrimer: Isolation and characterization of an *Arabidopsis thaliana* G protein gamma-subunit cDNA. Proc. Natl. Acad. Sci. USA **97,** 14784–14788.

Mason, M.G., and Botella, J.R. (2001). Isolation of a novel G-protein gamma-subunit from *Arabidopsis thaliana* and its interaction with Gbeta. Biochim. Biophys. Acta **1520,** 147–153.

Maxfield, F.R., and McGraw, T.E. (2004). Endocytic recycling. Nat. Rev. Mol. Cell Biol. **5,** 121–132.

McLaughlin, J.E., and Boyer, J.S. (2004). Glucose localization in maize ovaries when kernel number decreases at low water potential and sucrose is fed to the stems. Ann. Bot. (Lond.) **94,** 75–86.

Menges, M., and Murray, J.A. (2002). Synchronous *Arabidopsis* suspension cultures for analysis of cell-cycle gene activity. Plant J. **30,** 203–212.

Moore, B., Zhou, L., Rolland, F., Hall, Q., Cheng, W.H., Liu, Y.X., Hwang, I., Jones, T., and Sheen, J. (2003). Role of the *Arabidopsis* glucose sensor HXK1 in nutrient, light, and hormonal signaling. Science **300,** 332–336.

Natesan, S.K., Sullivan, J.A., and Gray, J.C. (2005). Stromules: A characteristic cell-specific feature of plastid morphology. J. Exp. Bot. **56,** 787–797.

Pandey, S., and Assmann, S.M. (2004). The *Arabidopsis* putative G protein-coupled receptor GCR1 interacts with the G protein alpha subunit GPA1 and regulates abscisic acid signaling. Plant Cell **16,** 1616–1632.

Perfus-Barbeoch, L., Jones, A.M., and Assmann, S.M. (2004). Plant heterotrimeric G protein function: Insights from *Arabidopsis* and rice mutants. Curr. Opin. Plant Biol. **7,** 719–731.

Pyke, K.A., and Howells, C.A. (2002). Plastid and stromule morphogenesis in tomato. Ann. Bot. (Lond.) **90,** 559–566.

Rensink, W.A., Pilon, M., and Weisbeek, P. (1998). Domains of a transit sequence required for in vivo import in *Arabidopsis* chloroplasts. Plant Physiol. **118,** 691–699.

Riou-Khamlichi, C., Menges, M., Healy, J.M., and Murray, J.A. (2000). Sugar control of the plant cell cycle: Differential regulation of *Arabidopsis* D-type cyclin gene expression. Mol. Cell. Biol. **20,** 4513–4521.

Rolland, F., Winderickx, J., and Thevelein, J.M. (2001). Glucose-sensing mechanisms in eukaryotic cells. Trends Biochem. Sci. **26,** 310–317.

Sheen, J., Zhou, L., and Jang, J.C. (1999). Sugars as signaling molecules. Curr. Opin. Plant Biol. **2,** 410–418.

Siderovski, D.P., and Willard, F.S. (2005). The GAPs, GEFs, and GDIs of heterotrimeric G-protein alpha subunits. Int. J. Biol. Sci. **1,** 51–66.

Skoglund, G., Basmaciogullari, A., Rouot, B., Marie, J.C., and Rosselin, G. (1999). Cell-specific localization of G protein alpha-subunits in the islets of Langerhans. J. Endocrinol. **162,** 31–37.

Smith, M.D., Fitzpatrick, L.M., Keegstra, K., and Schnell, D.J. (2002). In vitro analysis of chloroplast protein import. In Current Protocols in Cell Biology, K.M. Yamada, ed (New York: John Wiley & Sons), pp. 11.16.11–11.16.21.

Soellick, T.-R., and Uhrig, J. (2001). Development of an optimized interaction-mating protocol for large-scale yeast two-hybrid analyses. Genome Biol. **2,** research0052.0051–research0052.0057.

Strand, A., Asami, T., Alonso, J., Ecker, J.R., and Chory, J. (2003). Chloroplast to nucleus communication triggered by accumulation of Mg-protoporphyrinIX. Nature **421,** 79–83.

Tiessen, A., Prescha, K., Branscheid, A., Palacios, N., McKibbin, R., Halford, N.G., and Geigenberger, P. (2003). Evidence that SNF1-related kinase and hexokinase are involved in separate sugar-signalling pathways modulating post-translational redox activation of ADP-glucose pyrophosphorylase in potato tubers. Plant J. **35,** 490–500.

Tu, C.J., Schuenemann, D., and Hoffman, N.E. (1999). Chloroplast FtsY, chloroplast signal recognition particle, and GTP are required to reconstitute the soluble phase of light-harvesting chlorophyll protein transport into thylakoid membranes. J. Biol. Chem. **274,** 27219–27224.

Ullah, H., Chen, J.G., Temple, B., Boyes, D.C., Alonso, J.M., Davis, K.R., Ecker, J.R., and Jones, A.M. (2003). The beta-subunit of the *Arabidopsis* G protein negatively regulates auxin-induced cell division and affects multiple developmental processes. Plant Cell **15,** 393–409.

Ullah, H., Chen, J.G., Wang, S., and Jones, A.M. (2002). Role of a heterotrimeric G protein in regulation of *Arabidopsis* seed germination. Plant Physiol. **129,** 897–907.

Ullah, H., Chen, J.G., Young, J.C., Im, K.H., Sussman, M.R., and Jones, A.M. (2001). Modulation of cell proliferation by heterotrimeric G protein in *Arabidopsis.* Science **292,** 2066–2069.

Vanderbeld, B., and Kelly, G.M. (2000). New thoughts on the role of the beta-gamma subunit in G-protein signal transduction. Biochem. Cell Biol. **78,** 537–550.

Vermeer, J.E., Van Munster, E.B., Vischer, N.O., and Gadella, T.W., Jr. (2004). Probing plasma membrane microdomains in cowpea protoplasts using lipidated GFP-fusion proteins and multimode FRET microscopy. J. Microsc. **214,** 190–200.

Versele, M., de Winde, J.H., and Thevelein, J.M. (1999). A novel regulator of G protein signalling in yeast, Rgs2, downregulates glucose-activation of the cAMP pathway through direct inhibition of Gpa2. EMBO J. **18,** 5577–5591.

Vierstra, R.D. (2003). The ubiquitin/26S proteasome pathway, the complex last chapter in the life of many plant proteins. Trends Plant Sci. **8,** 135–142.

von Heijne, G. (1992). Membrane protein structure prediction. Hydrophobicity analysis and the positive-inside rule. J. Mol. Biol. **225,** 487–494.

Wang, Q., Sullivan, R.W., Kight, A., Henry, R.L., Huang, J., Jones, A.M., and Korth, K.L. (2004). Deletion of the chloroplast-localized Thylakoid formation1 gene product in *Arabidopsis* leads to deficient thylakoid formation and variegated leaves. Plant Physiol. **136,** 3594–3604.

Wang, X.Q., Ullah, H., Jones, A.M., and Assmann, S.M. (2001). G protein regulation of ion channels and abscisic acid signaling in *Arabidopsis* guard cells. Science **292,** 2070–2072.

Weiss, C.A., Garnaat, C.W., Mukai, K., Hu, Y., and Ma, H. (1994). Isolation of cDNAs encoding guanine nucleotide-binding protein beta-subunit homologues from maize (ZGB1) and *Arabidopsis* (AGB1). Proc. Natl. Acad. Sci. USA **91,** 9554–9558.

Xiao, W., Sheen, J., and Jang, J.C. (2000). The role of hexokinase in plant sugar signal transduction and growth and development. Plant Mol. Biol. **44,** 451–461.

Yang, P., Fu, H., Walker, J., Papa, C.M., Smalle, J., Ju, Y.M., and Vierstra, R.D. (2004). Purification of the *Arabidopsis* 26 S proteasome: Biochemical and molecular analyses revealed the presence of multiple isoforms. J. Biol. Chem. **279,** 6401–6413.

Zhao, J., and Wang, X. (2004). *Arabidopsis* phospholipase Dalpha1 interacts with the heterotrimeric G-protein alpha-subunit through a motif analogous to the DRY motif in G-protein-coupled receptors. J. Biol. Chem. **279,** 1794–1800.